#### Log Number: 163

# EXPERIMENTAL AND NUMERICAL INVESTIGATION OF AN ENTRANCE BLOCKAGE OF AN INNER CHANNEL IN DUAL-COOLED ANNULAR NUCLEAR FUEL

C. H. Shin, T. H. Chun, D. S. Oh and W. K. In<sup>1</sup>

<sup>1</sup> Korea Atomic Energy Research Institute, Daejeon, Korea <a href="mailto:shinch@kaeri.re.kr">shinch@kaeri.re.kr</a>, thchun@kaeri.re.kr, dsoh1@kaeri.re.kr, wkin@kaeri.re.kr

#### Abstract

A dual-cooled annular nuclear fuel for a Pressurized Water Reactor (PWR) has been introduced for a significant increase in reactor power. The Korea Atomic Energy Research Institute (KAERI) has been researching the development of a dual-cooled annular fuel for a power increase in an optimized PWR in Korea, OPR-1000. The main advantage of a dual-cooled annular fuel is an increased heat transfer area and a reduction in the fuel temperature, which would result in reduced fission gas release and increased fuel melting margin and Departure from Nucleate Boiling (DNB) margin.

The annular fuel rod is configured to allow the coolant flow through the inner channel as well as outer channel. Since the inner channel is isolated from the neighbor channels unlike the outer channels, an inner channel blockage is one of the principal technical issues of a dual-cooled annular fuel. Due to a partial blockage, the inner channel may be faced with a DNB accident.

A conceptual design used to complement the entrance blockage of an inner channel was suggested by KAERI. The through holes in this design are formed on a cylindrical wall of the lower end plug. When the inner channel is blocked by debris, coolant for the inner channel will be supplied through the side holes. But due to very unusual shape of the lower end plug, it is difficult to estimate the flow resistance of the side flow holes using empirical correlations available in the open literatures.

Experimental and Computational Fluid Dynamics (CFD) studies were performed to investigate the bypass flow through the side holes of the lower end plug to complement the entrance blockage of an inner channel. The form loss coefficient in the side holes was also estimated by using the pressure drop along the bypass flow path and DNB Ratio (DNBR) margin was estimated by a subchannel analysis code.

### 1. Introduction

Pressurized Water Reactor (PWR) is a main reactor type of electricity generation all over the world. It is believed at this moment that it will continue for the rest of this century. Given this situation, we still need to continue fuel R&D activity for this reactor type. A dual-cooled annular fuel rod for a pressurized water reactor has been introduced for a significant increase in reactor power.[1] The Korea Atomic Energy Research Institute (KAERI) has been researching the development of a dual-cooled annular fuel rod for a power increase of 20% in an optimized PWR in Korea, OPR-1000 [2, 3].

Several thermal-hydraulic tasks exist for the application of the dual-cooled annular fuel to OPR-1000. The primary task is to balance the Minimum DNBR (MDNBR) between the inner and outer channels since the coolant flows through the circular inner channel of annular fuel as well as the outer channels formed between the fuel rods. The MDNBR balance has been known to largely dependent on the thermal conductance in the inner and outer gaps [4].

Another task is to evaluate the operating condition that the inner coolant channel is partially blocked. The inner channel is isolated unlike the outer coolant channel which is opened to other neighbour outer channels for coolant exchange in the reactor core. If the inner channel is, as in a hypothetical event, completely blocked by the debris like wires, metal chips, and flat straps during normal operation, then the inner cladding may experience a rapid temperature increase because of no further coolant supply. Eventually, it could cause the Departure from Nucleate Boiling (DNB) at the inner channel and reach the Critical Heat Flux (CHF) condition, which means a fuel failure. Therefore, some remedy to avoid such an accident is indispensable for the safety of the annular fuel.

The new lower end plugs for the annular fuel [5, 6] were suggested to provide alternative flow paths in addition to the center entrance of the inner channel. The end plugs have the perforated flow holes on the side surface of long annular end plug body. It is expected, at least, to allow a minimum coolant supply to prevent the DNB occurrence at the inner channel in the case of partial or even complete blockage of the inner channel entrance. But due to very unusual shape of the lower end plug, it is hard to estimate the flow resistance of the side flow holes using empirical equations available in the open literature. Thus, it demands an experimental investigation to assure its function.

For the development of optimized end plugs, the Computational Fluid Dynamic (CFD) is a good alternative method for reduction of time and cost for experimental approach. The CFD analysis is applied to estimate and validate this preliminary test. In this paper, experimental and CFD studies were performed to investigate the bypass flow through the side holes of the end plug in the case of complete entrance blockage of the inner channel. The form loss coefficient in the side holes was also estimated by using the pressure drop along the bypass flow path.

This study calculated the MDNBRs in the inner and outer channels of a dual-cooled annular fuel rod. A subchannel analysis method is used to perform the thermal-hydraulic calculation for a reactor. A computational code, MATRA-AF, is developed to predict the thermal-hydraulic parameters for the annular fuel core [7]. The limit for the flow blockage in an inner channel is estimated based on the DNBR analysis.

# 2. Experimental setup and results

# 2.1 Experimental setup and test conditions

The long lower end plugs for the annular fuel rod were suggested to provide alternative flow paths in addition to the center entrance of the inner channel. One of the new end plugs is shown in Figure 1. Those are four perforated holes on the side surface of the long annular end plug body. When the inner channel is blocked by debris, coolant for the inner channel will be supplied through the side holes.

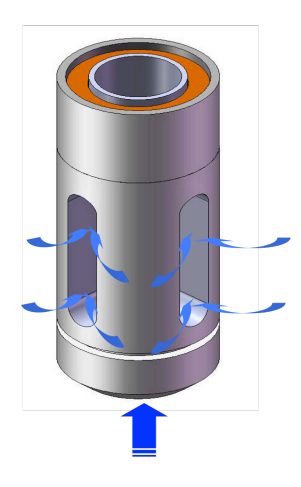


Figure 1 Schematic diagram of a lower end plug with side holes

Figure 2 shows a test loop to conduct the pressure drop measurement for the long end plug with side holes. The loop is composed of several components like test section, pump, flow-meter, flow control and bypass valves and water storage reservoir. Water is circulated through the test section in upward direction.

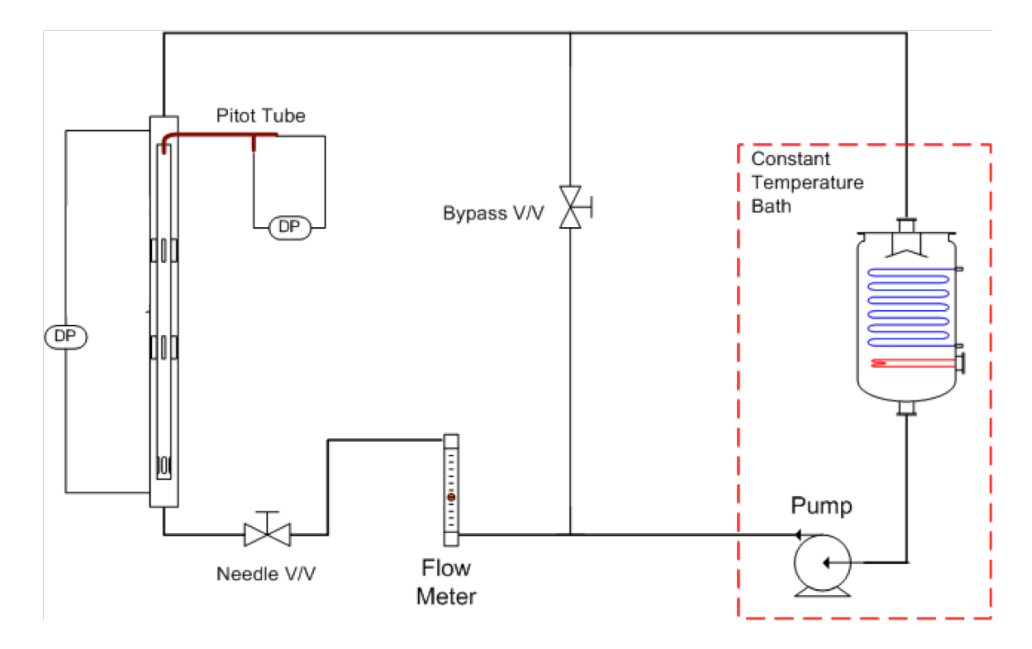


Figure 2 Schematic diagram of the experimental loop

The test section is a transparent 800 mm long and 25 mm diametric tube containing an annular metal rod with fins to simulate the spacer grid as well as to maintain the gap between rod and outside tube. The annular rod has inside and outside diameters of 8.4 mm and 15.9 mm, respectively and two sets of three fins are attached at the axial locations of 150 mm and 550 mm from the bottom of the rod. The long lower end plug is also installed at the bottom end of the rod. Each side hole has a dimension of a 3 x 6 mm<sup>2</sup> rectangular with two 3 mm diameter hemispheres at both ends. A total area of side holes is about 180 % of the center entrance area.

Experiments were conducted at atmospheric pressure and temperature. Flowrate of the loop is measured by a flow meter in the loop. Pressure drop is measured over the region of the annular rod. The maximum flowrate is  $20.0 \ \ell/min$  which corresponds to the Reynolds number of about  $5.0 \times 10^4$ .

The water entering the test section can be divided into inner and outer channel of the annular rod and merged again after leaving the annular rod. However, the outer channel in this experiment is plugged at just upstream of two fin locations to measure the inner channel flowrate directly.

The measurement uncertainty analysis is based on the description by Kline and McClintock[8]. The accuracy of the measured loss coefficient depends on the accuracy of the volume flow measured by the rotameter and the pressure drop measured by pressure transmitter. The calibration uncertainty of the pressure transmitter is 0.05% and the maximum random uncertainty was estimated below 2.35%. The accuracy of the rotameter is comparatively higher as 5%. The total measurement uncertainty for the loss coefficient of the side holes is below 13.1% for all experiments which have been carried out in this study.

# 2.2 Experimental results

A form loss coefficient of the side holes in the long lower end plug,  $K_{side}$  is defined as follows:

$$K_{side} = \Delta P_{side} / (\frac{1}{2} \rho V^2)$$
 (1)

Since the outer channel was blocked in the experiments, a balance of hydrodynamics could be expressed along the streamline:

$$\Delta P = (K_{in} + K_{side} + f \cdot L/d + K_{exit}) \cdot (\frac{1}{2} \rho v^2)$$
 (2)

The total pressure drop,  $\Delta P$  over the whole length includes a form loss of sudden contraction at outer channel entrance, a form loss through the side hole, friction loss on the inner channel surface and a form loss of inner channel exit. Here, it has to be noticed that all the form loss coefficients are defined on the velocity head of inner channel. From the test section geometry, the form loss coefficient for sudden contraction at the outer channel entrance,  $K_{in}$  is taken from simple abrupt change of flow area, and the form loss of inner channel exit,  $K_{exit}$  is taken from sudden expansion of a flow having a uniform velocity distribution[9];

$$K_{in} = 0.25 \text{ at Re} > 10^4$$
 (3)

$$K_{exit} = 0.8 \text{ at Re} > 3.5 \times 10^2$$
 (4)

For the friction loss in the inner channel, the friction factor, f was calculated by Blasius correlation as follows:

$$f = 0.316 \cdot \text{Re}^{-0.25} \tag{5}$$

The total loss coefficient was calculated by equation (2) from the measured total pressure drop and inner channel velocity. Then the loss coefficient of the side hole,  $K_{side}$  could be determined by equation (1) as follows:

$$K_{side} = \Delta P / (\frac{1}{2} \rho v^2) - (K_{in} + f \cdot L/d + K_{exit})$$
 (6)

The loss coefficient of side holes is summarized in Table 1 and is compared with CFD results in Figure 6. The averaged loss coefficient of whole experiments is 2.38, and the loss coefficients in the low Reynolds number are slightly higher.

Re	K					
	Total	friction	inlet	exit	side hole	
17,631	6.08	2.29	0.25	0.8	2.75	
22,668	5.87	2.15	0.25	0.8	2.67	
27,706	5.40	2.04	0.25	0.8	2.31	
32,743	5.38	1.96	0.25	0.8	2.37	
37,780	5.15	1.89	0.25	0.8	2.21	
42,818	5.18	1.83	0.25	0.8	2.30	
47,855	5.01	1.78	0.25	0.8	2.18	
50,374	5.02	1.76	0.25	0.8	2.22	

Table 1 Loss coefficients of side holes

# 3. CFD setup and results

# 3.1 CFD setup and calculation conditions

To estimate and validate this preliminary test, CFD analysis was applied. CFD analysis will be applied to decide geometry of test section and the test matrix for a next experiment, which will be more detail and accurate measurement. The CFD analysis has been performed by using CFD-ACE (Ver. 2003) code[10], a commercial CFD code based on a control volume method. The geometry for the CFD analysis is generated as same as experimental test section except inlet and outlet shapes. Inlet and Outlet of test section are suddenly expanded and contracted to be connected with flow line from test section outer diameter 35 mm to flow pipe diameter 20mm. In the CFD, these contraction and expansion are neglected and the inlet is expanded to upstream to make developed flow condition at the entrance of end plug. The mesh generation around the side hole is shown in Figure 3.

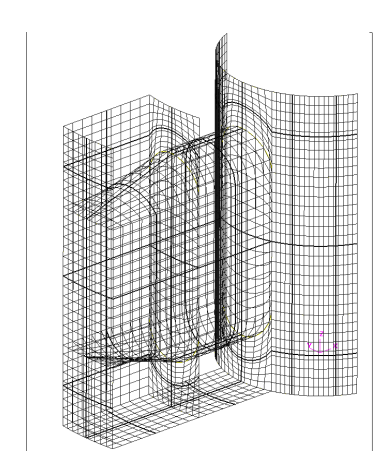


Figure 3. Grid generation around a side hole

The inlet boundary condition used the uniform velocity and a pressure boundary condition was applied at the outlet with constant pressure in the cross section of the exit. A no-slip condition was used at the rod surface and the grid spacer. The inlet blockage was modeled as a thin wall. The standard k- $\epsilon$  model of Launder and Spalding[11] is used for a turbulence model since it is practically useful and converges well for the complex turbulent flow.

## 3.2 Comparison with Experimental Results

To validate the CFD results, the outer channel was simulated to be completely closed as for the experiment. The velocity vector in the Re = 57,000 defined by inner channel exit velocity is shown in Figure 4. Since the inner channel blockage was modeled by thin-wall boundary condition at the inlet, recirculation regions appear at the inlet region from thin-wall to start of side holes and a pressure distribution is rapidly changed around end of side holes.

The plane averaged pressure results of CFD for total axial height and the inlet region are shown in Figure 5. As shown in figure, the axial pressure is suddenly dropped by the sudden contraction at the test rod inlet and the secondary pressure drop appears at the side hole end region. The pressure is slightly recovered after the side hole, and gradually decreased along the inner channel. To decide a pressure loss coefficient at the side holes region, a pressure drop between the upstream and downstream of the side holes is necessary. For an upstream pressure (P1), the values from end tip of a test rod to start of side holes are averaged and the downstream (P2) is a pressure at the fully recovered plane.

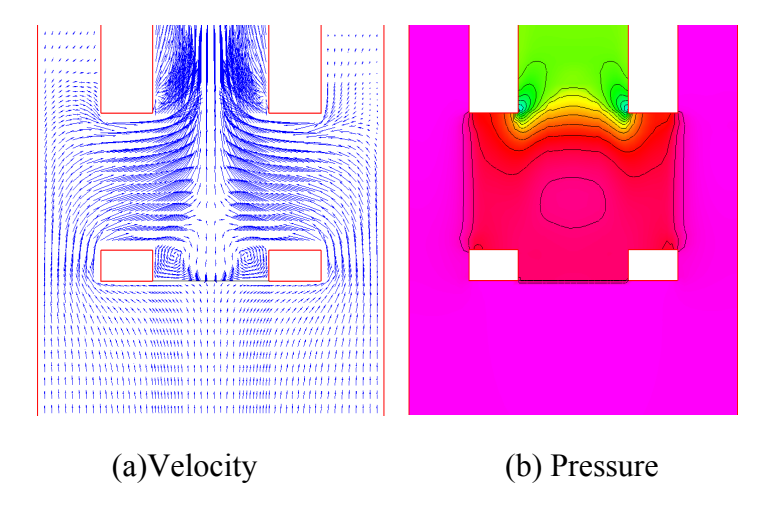


Figure 4 Velocity vector and pressure contour around the side holes

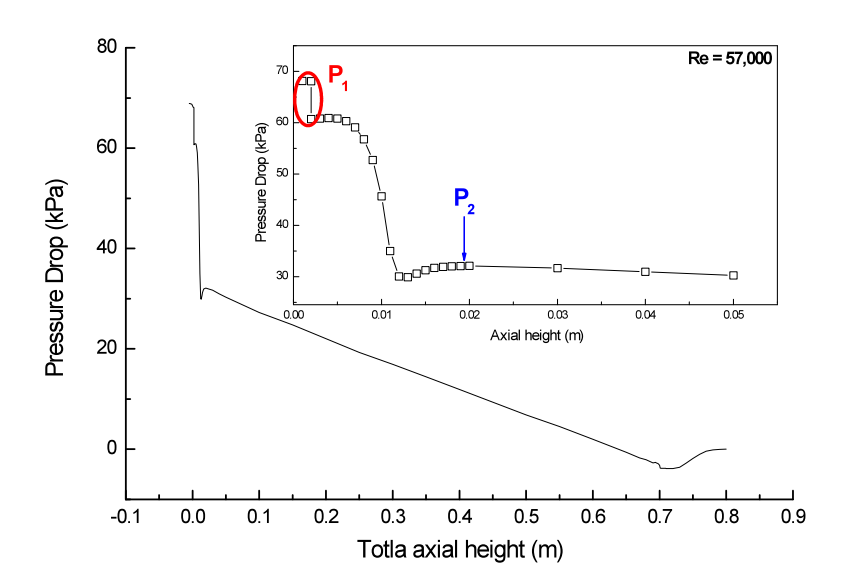


Figure 5 Pressure drop along axial direction without outer channel flow

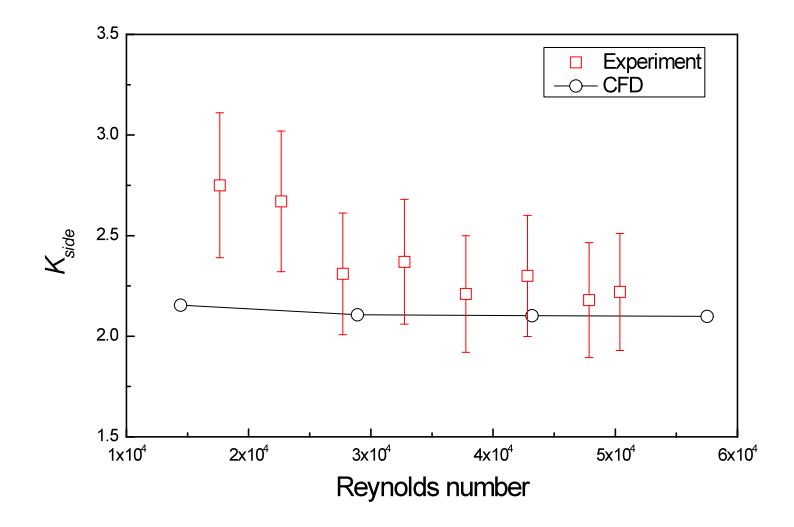


Figure 6 Comparison of experiment and CFD without outer channel flow

The loss coefficient as function of a velocity is illustrated with experimental results in Figure 6. The loss coefficient of side hole is calculated from the following equation as

$$K_{side} = (P_1 - P_2) / (\frac{1}{2} \rho v^2)$$
 (7)

The reference velocity is an exit velocity at the inner channel outlet. The comparison shows that the pressure loss coefficient is slightly underestimated by the CFD simulation below Re = 25,000, and total predicted results are underestimated about 10%. However the CFD results above Re = 25,000 are in good agreement with experiments within the uncertainty range, although this present measurement is carried out in a limited range up to Re = 50,000. The averaged loss coefficients above Re = 25,000 of experiments and CFD results are 2.27 and 2.10, respectively and then the difference of between both results is about 7.5%. From this comparison, the possibility of CFD analysis to derive loss coefficient of side flow hole for the long lower end plug is confirmed.

The side hole blockage effects are estimated for the outer channel close condition as shown in Figure 7. The loss coefficient was estimated for a velocity of an inner channel and a velocity of flow through a single hole. In the outer channel close condition, water flows into side holes and out inner channel exit. Therefore, the blockage of side hole leads to high loss coefficient at the same exit velocity. However, since the velocity through a side hole is increased as blockage, the loss coefficient for the single hole velocity shows opposite trend. Idelchik[9] suggested the loss coefficient of entrance into a straight circular tube through a side orifice in Diagram 3-16 is increased as increasing number of orifices from 1 to 2. And the loss coefficient depends on an area ratio of orifice to tube inner channel. When the area ratio of our design is 0.45, the increasing ratio of loss coefficient with increasing side hole is about 21% as increasing single to two orifices. In the figure, the increasing ratio for single to two orifices is about 30%. It is considered reasonable since the loss coefficient is a function of a side hole shape.

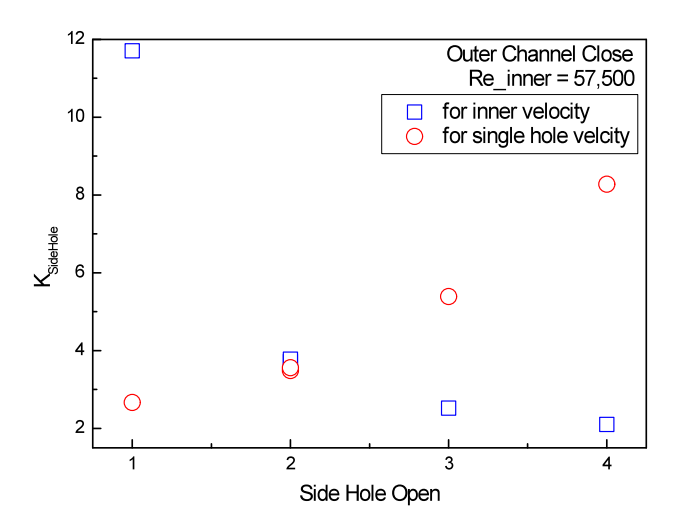


Figure 7 Loss coefficients of side holes for blockage of holes

# 4. MDNBR of flow blockage

A subchannel analysis method is used to perform the thermal-hydraulic calculations for the OPR1000 core. A computational code, MATRA-AF, is developed to predict the thermal-hydraulic parameters for the annular fuel core. The MATRA-AF code consists of MATRA module and annular fuel module. The MATRA module [12] is a subchannel analysis code which was developed to analyze the thermal-hydraulic characteristics in fuel bundle for a PWR. The annular module is developed to calculate the flow and heat splits in the inner and outer channels of annular fuel. The MATRA-AF code is therefore able to calculate the DNBR in the inner and outer channels as well as the flow and heat splits.

### 4.1 MDNBR Balance in the Dual-Cooled Fuel

Based on the lumped quadrant core model and the subchannel analysis parameters, the DNBR calculation for the 12x12 annular fuel was conducted by using the MATRA-AF code over the operable range of the gap conductance in order to determine its allowable range for the MDNBR not to exceed the DNBR limit. The DNBR limit is 1.30 which is typical value of specified acceptable fuel design limit for a PWR. The gap conductance changed from 3000 W/m<sup>2</sup> °C to 8500 W/m<sup>2</sup> °C for the inner gap and 6000 W/m<sup>2</sup> °C to 20000 W/m<sup>2</sup> °C for the outer gap. For the prediction of DNB, W-3 CHF correlation [13] was applied because this correlation is available for the wide range and the presence or absence of spacer grid in an inner and outer channel can be applied at the same time by the grid spacer factor in this correlation .

The calculated MDNBR values in the inner channel are listed in Table 2 for various combination of inner and outer gap conductance. It can be seen that the MDNBR increases in the inner channel and decreases in the outer channel as the outer gap conductance ( $h_{go}$ ) increases. The MDNBR in the inner channel is lower than the DNBR limit for the case of the outer gap conductance being smaller than twice the inner gap conductance ( $h_{gi}$ ), i.e.,  $h_{go} < 2h_{gi}$ . However,

the MDNBR in the outer channel was always higher than the DNBR limit for any gap conductance examined.

Table 2 MDNBR values in the inner channel at 120% power with 118% overpower depending on the inner and outer gap conductance (h<sub>ci</sub>, h<sub>co</sub>)

depending on the inner and outer gap conductance $(n_{gi}, n_{go})$						
	$h_{go} = 6000$	7000	10000	14000	20000	
$h_{gi} = 3000$	1.993	2.345	3.030	3.494	3.783	
3500	1.489	1.816	2.493	3.000	3.350	
4500	-	1.108	1.722	2.213	2.605	
6500	-	-	0.881	1.288	1.650	
8500	-	-	-	0.814	1.133	

Figure 8 illustrates the allowable range of the inner and outer gap conductance in which the MDNBR is higher than the DNBR limit. It shows a significant increase of the operable region as the outer gap conductance increases. The outer gap conductance should be greater than 4000 W/m<sup>2</sup> °C while the inner gap conductance be smaller than approximately 7000 W/m<sup>2</sup> °C. It is also noted in Figure 8 that the MDNBR in the inner and outer channels is well balanced if the ratio of outer and inner gap conductance ( $h_{go}/h_{gi}$ ) is in between 2 and 3.

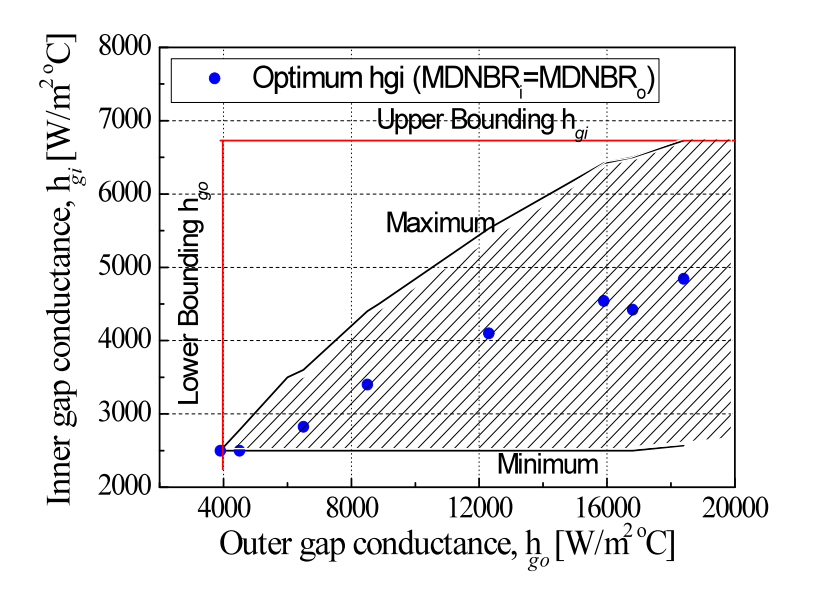


Figure 8 Acceptable range of the gap conductance.

## 4.2 Flow Blockage of the Inner Channel

The isolated inner channel of the dual-cooled fuel is facing a question for a hypothetical flow blockage. The MDNBR is calculated for various partial blockages by adjusting the form loss coefficient at the entrance of the inner channel. The entrance form loss coefficient was gradually increased from 0.4 (no blockage) until the MDNBR dropped below the DNBR limit (1.30).

Figure 9 shows the effect of entrance blockage on MDNBR and coolant mass flux in the inner channel. As the blockage increased, the mass flux decreased significantly due to the whole core flow redistribution to accommodate equal pressure drops across each channel. The MDNBR also decreased due to the decreased mass flux. The calculated MDNBR is 1.709 and 1.207 for 55% and 60% blockages, respectively. The maximum blockage of flow area in the inner channel should be therefore smaller than 55% for the MDNBR not to drop below 1.30.

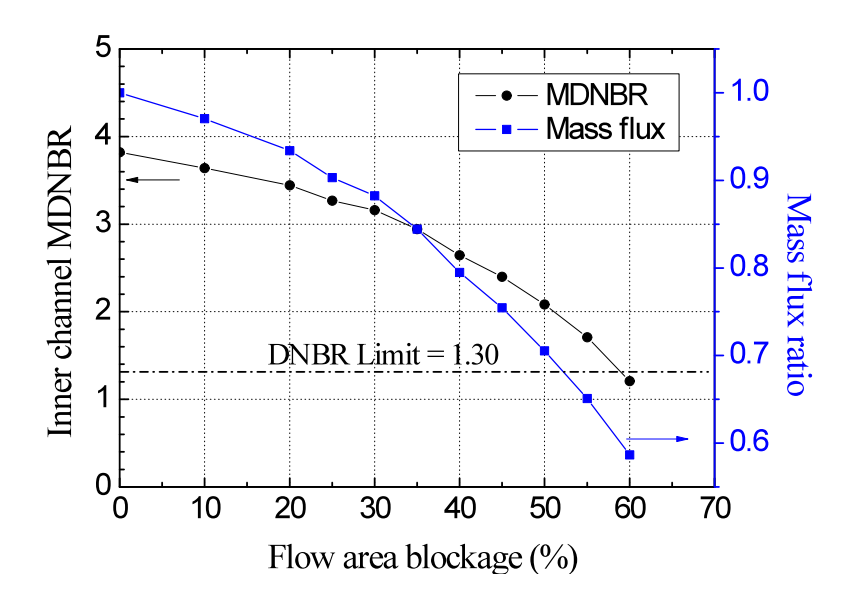


Figure 9 Flow blockage dependent MDNBR in the inner channel.

## 5. Conclusion

A long lower end plug with side holes as the alternative flow path was proposed for the dual cooled annular fuel in order to avoid the occurrence of CHF even in the case of complete blockage at the entrance of the inner channel, as a hypothetical event.

An experiment with single annular fuel within a round tube was performed to measure the form loss coefficient of the side holes in the long lower end plug. A CFD analysis was performed to estimate the loss coefficient and compare with the experiment. The CFD simulations will be useful to decide geometry of test section and the test matrix for the future experiment, which will be more accurate measurement.

Log Number: 163

The possibility of CFD analysis to derive loss coefficient of side flow hole for the long lower end plug is confirmed. The CFD results are in good agreement with experiments within the uncertainty range.

When outer channel flow is considered and the spacer grids of an outer channel are neglected, the outer channel flow rate is much larger than an inner channel for pressure balance between both channels. The loss coefficient of side holes decreases as outer channel blockage ratio increases. To define a loss coefficient of side flow holes with outer channel flow, the major parameters such as inner and outer channel velocity, loss coefficient of spacer grids, and exit form loss coefficient should be measured.

A thermal-hydraulic analysis using the subchannel method was performed to calculate the MDNBR depending on the gap conductance and the entrance blockage in an inner channel. It was found that the MDNBR in the inner and outer channels is well balanced if the ratio of outer and inner gap conductance is in between 2 and 3. The acceptable range of the gap conductance was significantly enlarged as the outer gap conductance increased. The maximum blockage of flow area in the inner channel was calculated to be approximately 55% for the MDNBR to be greater than the DNBR limit.

Consequently, it is concluded that the long end plug with side holes can provide the coolant flow to the inner channel even in the complete blockage of main entrance. However, it is necessary to optimize the side hole (size, shape and quantity) from the experimental and numerical studies in the future.

# Acknowledgements

The authors would like to express their appreciation to the Ministry of Science and Technology of Korea for its financial support.

#### References

- [1] M. S. Kazimi, "Introduction to the annular fuel special issue," Nuclear Technology, Vol. 160, 2007
- [2] T. H. Chun, "A Potential of Dual Cooled Annular Fuel for OPR-1000 Power Uprate," <u>Proceedings of 2009 LWR Fuel Performance</u>, Paris, France, 2009 Sept. 6-10
- [3] C. H. Shin, W. K. In, D. S. Oh, and T. H. Chun, "The Design of Annular Fuel Array for a High-Power-Density PWR," <u>Transactions of the KNS Autumn Meeting</u>, Gyeongju, Korea, 2009 Oct. 29-30
- [4] C. H. Shin, W. K. In, D. S. Oh, and T. H. Chun, "DNBR Analysis of a Dual-Cooled Annular Fuel for the OPR-1000 Application," <u>Transaction of the KNS Spring Meeting</u>, Pyeongchang, Korea, 2009 May 27-28.
- [5] D. S. Oh, et al., "Lower and Upper End Plugs of an Annular Fuel Rod," US Patent, US 7,711,079 B2, May, 2010
- [6] T. H. Chun, et al., "Annular Fuel Lower End Cap to Prevent Blockage of Inner Channel Flow by the Debris," Korea Patent, 2009-0134235, 2009

- [7] C. H. Shin, K. W. Seo, and T. H. Chun, "A Parametric Study on the Thermal Hydraulic Design for an Annular Fuel Assembly," <u>Transactions of the KNS Autumn Meeting</u>, Pyeongchange, Korea, 2008 Oct. 30-31.
- [8] S. J. Kline and F. A. McClintock, "Describing uncertainty in single-sample experiments," Mechanical Engineering, vol. 75, pp 3-8, 1953
- [9] I. E. Idelchik, "Handbook of Hydraulic Resistance, 2<sup>nd</sup> Edition," Hemisphere Publishing Corporation, 1986
- [10] CFD-ACE, Version 2003, CFD Research Corporation, Huntsville, Alabama.
- [11] B. E. Launder and D. B. Spalding, "The Numerical Computation of Turbulent Flows," Comp. Methods for Appl. Mech. Eng. Vol. 3, pp 269-289, 1974
- [12] Y. J. You, D. H. Hwang and D. S. Sohn, "Development a Subchannel Analysis Code MATRA Applicable to PWRs and APWRs," Journal of Korean Nuclear Society, Vol. 31, pp314-327, 1999
- [13] L. S. Tong and Y. S. Tang, "Boiling Heat Transfer and Two-Phase Flow, 2<sup>nd</sup> Edition," Taylor & Francis, 1997